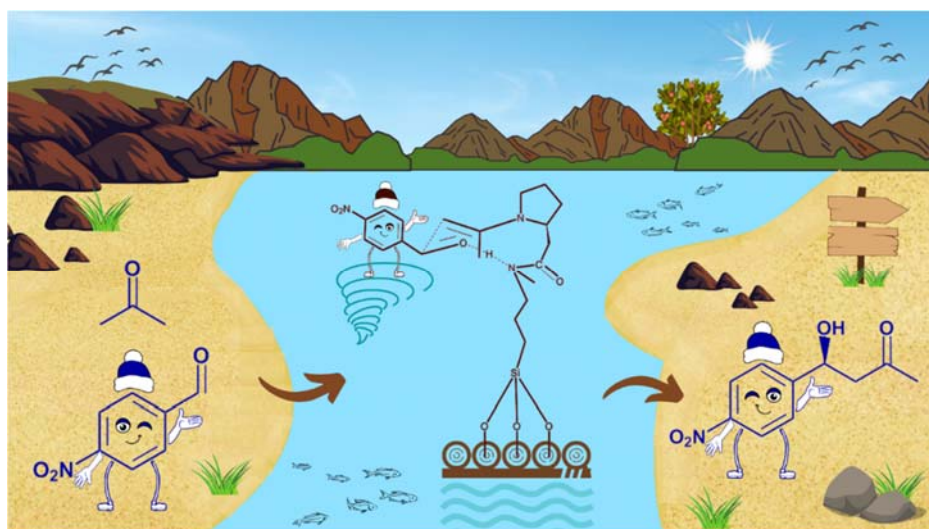*Spick-and-span protocol for designing of silica-supported enantioselective organocatalyst for the asymmetric aldol reaction*

2.1 Introduction:

Enantiomerically active compounds are highly precious scaffolds and have garnered great attention in recent years. These compounds have been found to be active in various ranges of research fields,[1] especially in the formulation of pharma products. Many contemporary medicinal drugs are chiral and require high levels of enantiopurity in clinical testing as demanded by governing bodies.[2] Therefore, there has been ancient attention to synthetic approaches providing non-racemic products and with current speedy growth in the catalytic asymmetric synthetic procedures.

For various asymmetric transformations especially in pharmaceuticals, a range of homogeneous catalysts has been used in the past decades.[3] Most of the preparative techniques reported so far are based on homogeneous modes that need excess loading of catalyst and strenuous purification techniques. On the other hand, enhancing catalytic potency and selectivity through dint of support synergism in heterogeneous catalysis is consistently remained an eye-catching approach, in particular, colossal exertions have been devoted towards the grafting of chiral organo-scaffolds on the solid supports for improving their catalytic competence and also to enable the recycling and reuse strategy of the catalyst. Despite the truth, the fairy turned out not to be real when it deals with asymmetric reactions.[4,5]

The foremost evidence of proline grafted on a solid support for asymmetric aldol synthesis dates back to the year 2003.[6] *L*-proline has been in limelight on account of its natural abundance as well as a metal-free substrate which signifies important consideration in terms of economy in pharmaceuticals. Benaglia and co-workers[4] have grafted *L*-proline onto a poly(ethylene glycol) (PEG) framework.[7–9] Polystyrene (beads),[10,11] Merrifield resin,[12] ionic liquids,[13–16] dendrimers[17] and multi-wall carbon nanotubes (MWCNTs)[18] are some other prevalent supports for *L*-proline. It always remains a confront particularly when mesoporous silica with flexible mesoporous surfaces, furnishes the best practicable solutions as support.[19–26] Based on the fascinating mass transfer reaction, higher surface area and the ease competence of grafting chiral organic scaffolds, mesoporous silica has been used as effectual support for *L*-proline and endures for alluring catalytic properties.[27–29]

To date, most of the reported methods for the synthesis of silica-supported *L*-proline catalysts involve multistep and somewhat complex syntheses, involving protecting/

deprotecting steps i.e. protections of the secondary amine of *L*-proline through t-butyloxycarbonyl (Boc) and carboxylic acid via esterification.[30] In contrast to this, E. Kristensen et al.[31] have reported polymer-supported proline as an organocatalyst utilizing unprotected proline, avoiding the protection/deprotection steps. In line with this, A. A. Elmekawy et al.[32] and Z. An et al.[33] have developed proline immobilized onto silica supports through a reaction between trans-4-hydroxy-*L*-proline and chloropropyl tethers not requirement for protecting groups. However, the downside of this process is to employ a very pricey organic substrate i.e., trans-4-hydroxy-*L*-proline. In the present work, In the current investigation, a remarkably effective and enantioselective catalyst has been synthesized by anchoring the *L*-proline chiral framework onto the silica matrix, denoted as *L*-proline-(3°amine)-*f*-SiO$_2$, eluding the protection/deprotection steps. The as-synthesized catalyst was weigh-up against the asymmetric aldol reaction, demonstrating exceptional performance. Notably, the reaction proceeded with 100% conversion and achieved an enantioselectivity of > 99% for the *S*-isomer. Additionally, the catalyst displayed remarkable stability, maintaining its activity over seven consecutive recycling cycles without any loss of efficiency.
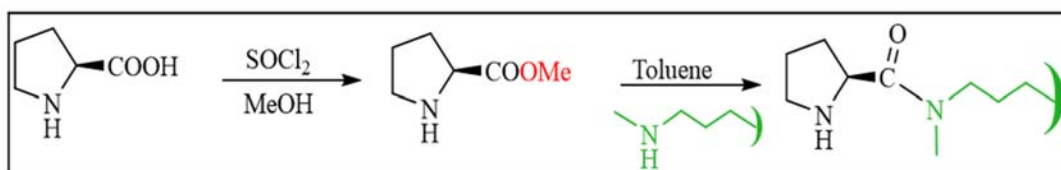
Scheme 2.1 Formation of the *L*-proline chiral scaffold attached to the SiO$_2$ matrix.

2.2 Experimental section

2.2.1 Synthesis of N-methyl-3-(trimethoxysilyl)propan-1-amine (NMAPTMS) grafted onto a silica matrix, CH$_3$NH-*f*-SiO$_2$:

A compound CH$_3$NH-*f*-SiO$_2$ was synthesized through a reported post-synthetic grafting method.[34] In this approach, pre-activated calcinated silica (1.0 g) was introduced to dry toluene (10 mL) within a round-bottomed flask (RBF). The blend was subsequently raised to a reflux temperature and maintained under continuous stirring for a duration of 1 hour within an argon atmosphere. Following this, NMAPTMS (2.05 mmol, 0.39 mL) was gradually added drop by drop, with stirring maintained in the same environment. The reaction proceeded for a duration

of 24 hours, after which the solid was filtered and subjected to sequential washing with toluene and acetone. The resulting solid material was subsequently dried at 120 °C in a vacuum oven for a period of 12 hours.

2.2.2 Synthesis of *L*-Proline methyl ester:

In this method, *L*-proline (8.7 mmol, 1g) was added to dry methanol (10 mL) and was kept untouched till the reaction mixture converted clear. Subsequently, the reaction mixture was cooled to a range of 0 to 5 °C, and thionyl chloride ($SOCl_2$) (9.5 mmol, 1.136 g) was carefully added drop by drop. Afterward, the mixture was subjected to stirring at room temperature throughout the entire night. Subsequent to this, the solvent was eliminated, and the resulting product was subjected to washing with ether. The product was then subjected to vacuum drying, yielding *L*-proline methyl ester in the Zwitterionic form, containing an amine. The aim is to require a free amine form; therefore, a basic condition was provided via the addition of a saturated solution of $NaHCO_3$ (sodium bicarbonate) in it and extracted the organic aliquots in the ethyl acetate solution. The excess solvent was removed through evaporation to get a pure product. The progress of the reaction was tracked using TLC with a solvent mixture of methanol and water (7:3).

2.2.3 Synthesis of *L*-proline grafted onto 2°amine-functionalized silica, *L*-proline-(3°amine)-*f*-SiO₂:

The substance CH_3NH-*f*-SiO_2 (1.0 g) was suspended within toluene (10 mL) and subjected to continuous stirring while being heated for 1 hour at a reflux temperature, all under an argon atmosphere. Following this, *L*-proline methyl ester (2.05 mmol, 0.264 g) was introduced into the reaction mixture under the previously mentioned conditions. The reaction was allowed to proceed for a span of 12 hours. Subsequently, the solid catalyst was separated through filtration, then rinsed successively with deionized water and ethanol. The resulting material was eventually dried in an air oven at 120 °C for a duration of 12 hours.

2.2.4 General reaction condition:

The effectiveness of the *L*-proline-(3°amine)-*f*-SiO$_2$ catalyst was evaluated in the context of an asymmetric aldol reaction. In this regard, a catalyst quantity of 0.5 g was combined with 4-nitrobenzaldehyde and acetone within a three-neck round-bottomed flask. The mixture was then allowed to equilibrate at 25 °C while being continuously stirred for a duration of 2 hours under an argon atmosphere. After the recovery of the catalyst through filtration, the conversion rate was determined using HPLC coupled with a UV detector to analyze the crude product. Additionally, the enantiomeric excess of the resulting product was gauged using chiral-phase HPLC analysis. The chiral-phase HPLC setup involved utilizing a Chiralpak OJ-H column.[35] Moreover, testing other aldehydes such as 4-Methyl benzaldehyde and benzaldehyde yielded lower results (i.e., 0.21% for 4-Methyl benzaldehyde and 1.01% for benzaldehyde) under the optimized conditions.

2.3 Results and discussion:

2.3.1 ^{13}C CP MAS NMR spectra
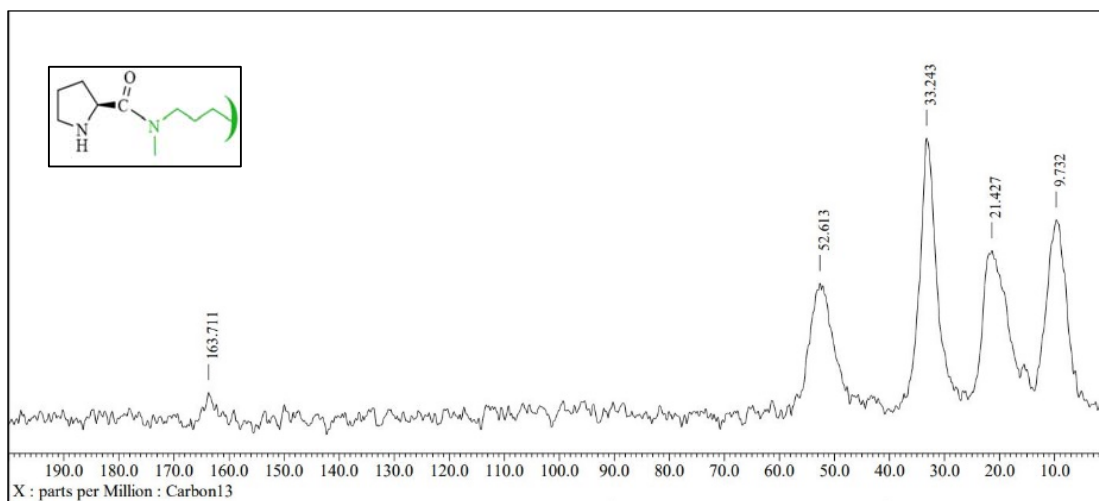
Figure 2.1 ^{13}C CP MAS NMR spectra of *L*-proline-(3°amine)-*f*-SiO$_2$.

A solid-state ^{13}C CP MAS NMR spectrum has been performed to provide chemical information regarding the condensation of CH$_3$NH-*f*-SiO$_2$ and *L*-proline organic scaffold. ^{13}C

CP MAS spectrum of the *L*-proline-(3°amine)-*f*-SiO$_2$ catalyst [*Figure 2.1*] showed a peak at 163.71 ppm corresponding to the carbonyl group, confirming the successful tethering of proline to the silica surface. The other peaks were observed at 52.61, 33.24, 21.43 and 9.73 ppm, which are assigned to the MAPTMS linker and proline ring.[33]

2.3.2 X-ray diffraction pattern
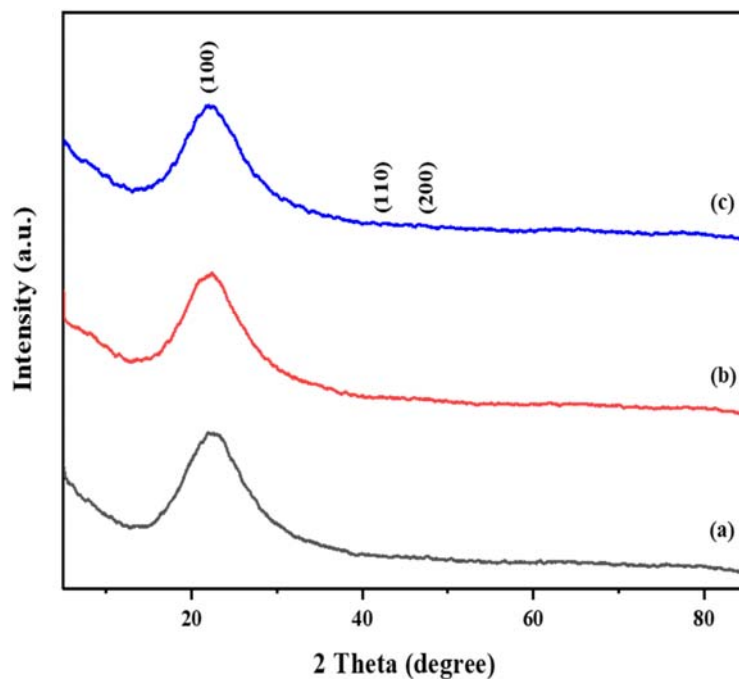
Figure 2.2 XRD patterns (a) pure silica (b) CH$_3$NH-*f*-SiO$_2$ (c) *L*-proline-(3°amine)-*f*-SiO$_2$.

The powder XRD is an imperative technique to determine the crystallinity of the as-prepared samples. XRD patterns of pure silica, CH$_3$NH-*f*-SiO$_2$ and *L*-proline-(3°amine)-*f*-SiO$_2$ are given in *Figure 2.2* For all the samples, typical 100, 110, and 200 reflections are observed, which can be assigned to the specific hexagonal arrays of 1-dimensional channel structures. This data confirms that the ordered structure is retained throughout the grafting procedure.[36]

2.3.3 Transmission electron microscopy
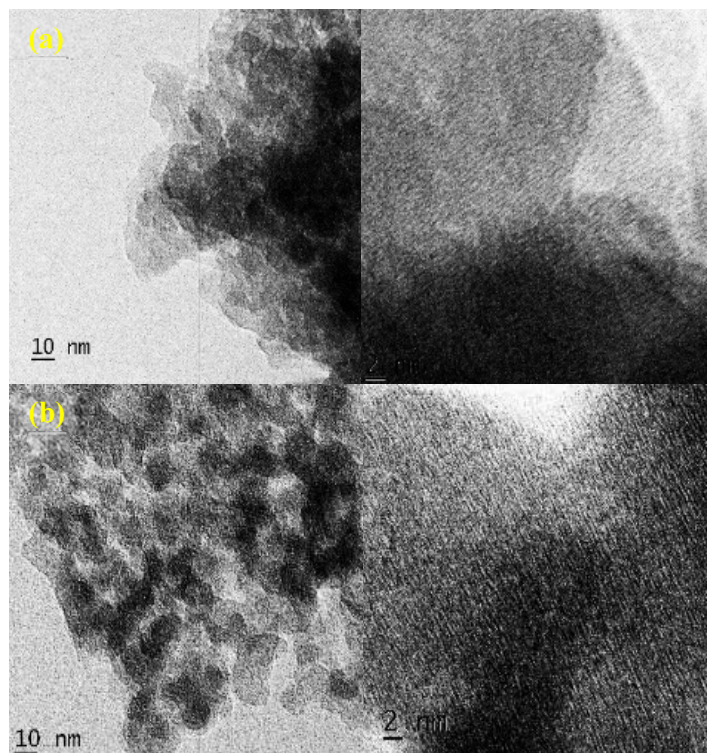
Figure 2.3 HR-TEM image (a) pure silica (b) *L*-proline-(3°amine)-*f*-SiO$_2$

HRTEM images of pure silica and *L*-proline-(3°amine)-*f*-SiO$_2$ catalyst are presented in *Figure 2.3*. Spherical or a more regular form of morphologies can be clearly observed [*Figure 2.3* (a)]. TEM images reveal that the structural arrangement of pristine silica remains unchanged following the introduction of organic modifications[*Figure 2.3* (b)].[37]

2.3.4 BET analysis
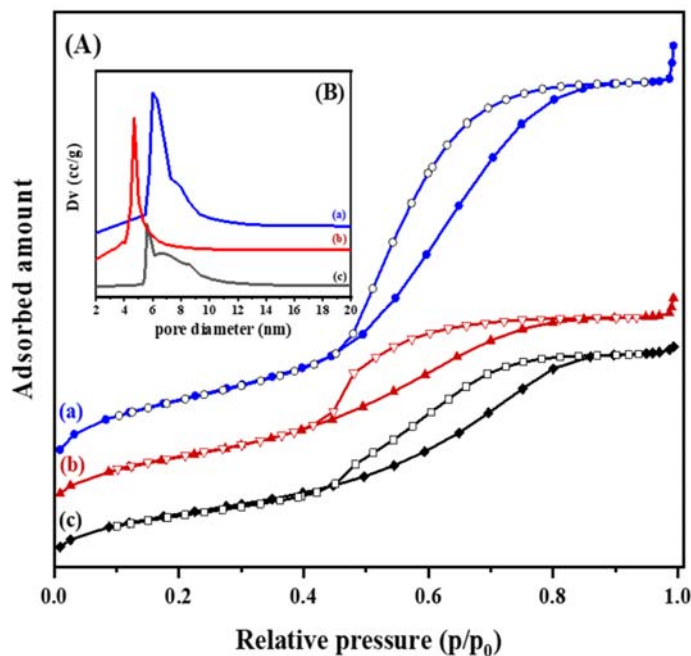
Figure 2.4 (A) N_2 adsorption−desorption isotherms of (a) pure silica (b) CH_3NH-*f*-SiO_2 (c) *L*-proline-(3°amine)-*f*-SiO_2 (B) BJH pore size distributions of (a) pure silica (b) CH_3NH-*f*-SiO_2 (c) *L*-proline-(3°amine)-*f*-SiO_2.

*Table 2.1* **Textural parameters of catalysts**

Sample	Surface area/m² g⁻¹	Pore volume/cm³ g⁻¹	Average pore diameter/nm
Pure silica	355.49	0.66	6.0
CH_3NH-*f*-SiO_2	197.03	0.30	4.7
L-proline-(3°amine)-*f*-SiO_2	184.12	0.30	5.6

Figure 2.4 (A) and (B) present the N_2 adsorption-desorption isotherms and BJH pore size distributions of pure silica, CH_3NH-*f*-SiO_2, and *L*-proline-(3°amine)-*f*-SiO_2 samples. Evidently, all three samples display type IV isotherms, indicative of the maintained ordered mesoporous configuration of the silica gel. The data in *Table 2.1* reveal a gradual reduction in

BET surface area, indicating the effective integration of these organic frameworks onto the silica matrix.[38]

2.3.5 FTIR spectra
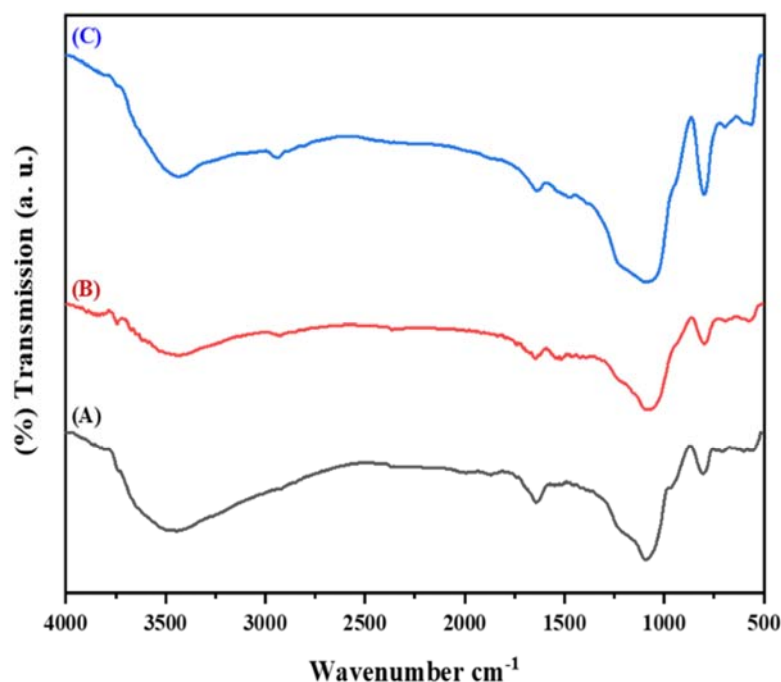
Figure 2.5 FTIR spectra of (A) pure silica (B) CH_3NH-*f*-SiO_2 (C) *L*-proline-(3°amine)-*f*-SiO_2.

Figure 2.5 shows the FTIR spectra of pure silica, CH_3NH-*f*-SiO_2 and *L*-proline-(3°amine)-*f*-SiO_2. FTIR spectrum of pure silica [*Figure 2.5* (A)] exhibited characteristic strong bands at 1094 and 804 cm^{-1}, these peaks were associated with the asymmetric and symmetric stretching vibrations of Si-O-Si bonds. Furthermore, a broad peak at 3444 cm^{-1} and a strong peak at 1643 cm^{-1} were assigned to surface -OH groups of mesoporous silica[39]. Successful functionalization with the MAPTMS linker was substantiated by rolling out of a new peak at 2924 cm^{-1} in the FTIR spectrum of CH_3NH-*f*-SiO_2 [*Figure 2.5* (B)] due to characteristics of -CH_2 stretching vibrations of the propyl chain. Besides this, the peak at 1643 cm^{-1} was shifted to 1645 cm^{-1} which confirms the formation of the –C-O-Si group.[40] Moreover, the intensity of surface hydroxyl groups at 3440 cm^{-1} was found to be receded as a result of the successful

functionalization of some of the –OH groups by the MAPTMS linker. On the other hand, in the FTIR spectrum of *L*-proline-(3°amine)-*f*-SiO$_2$, very infirm bands at 3434, and 1642 cm^{-1} are observed, which can be assigned to N–H (secondary amine) stretching, and C=O group, respectively of *L*-proline.[37] The weak intensity of these peaks could be attributed to the comparatively low concentration of proline attached to the silica matrix through the MAPTMS linker.

2.3.6 Elemental analysis

Quantification of the elements loaded in silica was performed using elemental analysis (CHN): Carbon, 5.92%; Hydrogen, 3.58% and Nitrogen, 2.53%. These results confirm that proline successfully was tethered via the MAPTMS linker onto the surface of silica.[36]

2.4 Catalytic activity:

The direct asymmetric aldol reaction catalyzed by *L*-proline-(3°amine)-*f*-SiO$_2$ is shown in *Scheme 2.2*
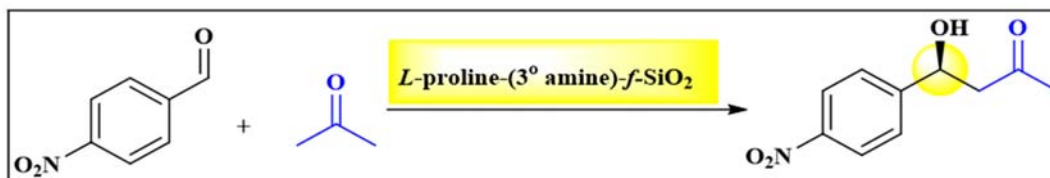
Scheme 2.2 Asymmetric aldol reaction catalyzed by *L*-proline-(3°amine)-*f*-SiO$_2$.

2.4.1 Effect of temperature

As shown in *Table 2.2*, the catalytic activity of the prepared catalyst was assessed through a comparison with asymmetric aldol reaction, employing varying temperatures and utilizing 4-nitrobenzaldehyde and acetone as initial substrates. It is clear from the *Table 2.2* that 100% conversion is achieved for the temperature range of 0 °C to 50 °C. however, the selectivity oscillates between 89.11% and 99.10% where the maximal selectivity (99.10%) is observed at a temperature of 25 °C which was considered as the preferred temperature for the further investigation.

Table 2.2 Effect of temperature on asymmetric aldol reaction.

Entry	Temperature/°C	Conversion (%) [a]	ee (%) [b]
1	0°C	100	97.48
2	25°C	100	99.10
3	RT (33°C)	100	95.56
4	50°C	100	89.11

[a] Conversion Determined by normal HPLC analysis. [b] ee Determined by chiral-phase HPLC analysis (Chiralpak OJ-H)
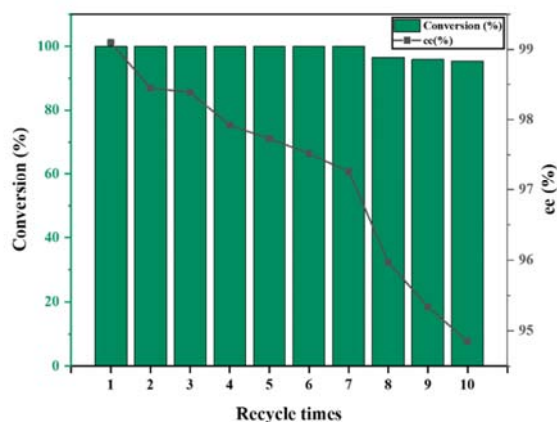
2.4.2 Recyclability test

The recyclability test is one of the imperative parameters apt to any heterogeneous catalytic system. Tethering of *L*-proline onto the silica matrix via MAPTMS linker makes the *L*-proline-(3°amine)-*f*-SiO$_2$ catalyst more stable in the reaction system. To examine the reusability for the direct asymmetric aldol reaction, the *L*-proline-(3°amine)-*f*-SiO$_2$ catalyst could be dexterously isolated from the reaction mixture by centrifugation. The overlaying organic part along with the product was separated from the underneath catalyst by effortless decantation, washed with ethanol several times and followed by oven drying overnight before employing for the next cycle. The reaction aliquot after each catalytic run was analyzed by HPLC with UV detector. The results of each catalytic run are tabulated in *Table 3* and are depicted in *Figure 2.6*. For the asymmetric aldol reaction, the conversions in a fresh to the seventh cycle remain completely invariable i.e., 100%, however, a bit by bit drop in the

selectivity (i.e., 99.10% in a fresh to 97.26% after 7th recyclability test) (*Table 2.3*, Entry 0 to 6) was observed. After the seventh cycle, the recycling of the *L*-proline-(3°amine)-*f*-SiO$_2$ catalyst resulted in a diminutive decrease in activity from 100% to 95.39% in the tenth cycle. Meanwhile ee% continuously dropped from 99.10% in the first cycle to 94.85% in the tenth cycle. To the gratification, the *L*-proline-(3°amine)-*f*-SiO$_2$ catalyst could be reused seven consecutive cycles with absolutely zero % loss in conversion with minute decrease in enantioselectivity of aldol product proved to be having excellent stability and reusability.

Table 2.3 Recyclability data of the asymmetric aldol reaction.

| Entry	Conversion (%) [a]	ee (%) [b]
0	100	99.10
1	100	98.45
2	100	98.39
3	100	97.92
4	100	97.73
5	100	97.52
6	100	97.26
7	96.48	95.97
8	95.88	95.34
9	95.39	94.85

[a] Conversion Determined by normal HPLC analysis. [b] ee Determined by chiral-phase HPLC analysis (Chiralpak OJ-H)

Figure 2.6 Recyclability test of *L*-proline-(3°amine)-*f*-SiO$_2$ catalyst over asymmetric aldol reaction.

2.5 Plausible catalytic pathway for the asymmetric aldol reaction.

The plausible reaction pathway for the asymmetric aldol reaction using the *L*-proline-(3°amine)-*f*-SiO₂ catalyst occurs via an enamine mechanism as shown in *Figure 2.7*.

(a) Favoured   (b) Unfavoured
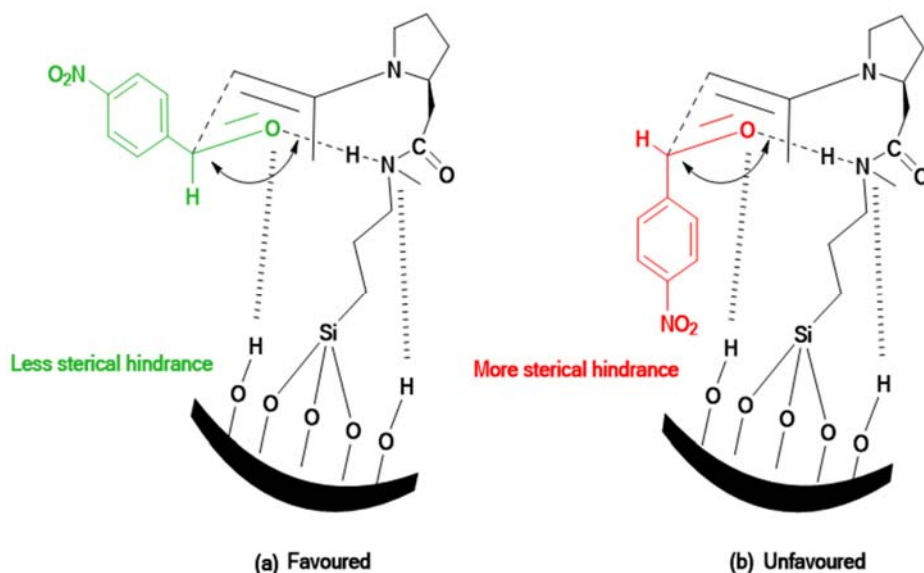
Figure 2.7 A plausible reaction pathway for the asymmetric aldol reaction using *L*-proline-(3°amine)-*f*-SiO₂.

There is a ubiquitous perception that *L*-proline-based supported catalysts show structure reversal. Z. An et al.[27] have indicated that the asymmetric aldol reaction between p-nitrobenzaldehyde and acetone, catalyzed by *L*-proline, predominantly yielded the *R* isomer. However, in the present study, the sole presence of the *S* isomer as the primary product was observed. According to the proposed mechanism by Z. An and colleagues, the aldehyde likely attacks the enamine of the ketone in the proline-catalyzed homogeneous asymmetric aldol reaction. The *re*-attack on the anti-enamine *R* isomer by transition states is expected to be energetically more favorable than the syn-enamine's *si*-attack by transition states, leading to the production of the *S* isomer as the major outcome. In contrast, in present research involves *L*-proline immobilized onto silica supports, specifically *L*-proline-(3°amine)-*f*-SiO₂, where the mesoporous channels play a crucial role. These channels hinder the *re*-attack on the anti-enamine, promoting the creation of an inverted configuration, as depicted in *Figure 2.7*. The

structure (a) exhibits more favorable than structure (b), possibly due to steric hindrance. The aldehyde becomes more electrophilic due to hydrogen bonding with an amine, as shown in *Figure 2.7*. The catalyst, *L*-proline-(3°amine)-*f*-SiO$_2$, offers stronger confinement because the amine group of the linker prefers to orient itself near the hydrophilic blocks. In the subsequent step, C-C bond formation ensues, leading to the predominant formation of the *S* isomer as the primary product.[33]

2.6 Conclusion

In conclusion, present study introduces an innovative approach for synthesizing an economical *L*-proline chiral scaffold integrated onto a silica matrix, bypassing the need for protection and deprotection procedures. This research presents a novel application of this synthesized catalyst in an asymmetric aldol reaction, eliminating the requirement for excessive organic solvents. The catalyst showcases remarkable efficacy, achieving complete conversion and an impressive enantioselectivity of *S*-isomer (> 99%). Additionally, present catalyst demonstrates exceptional recyclability, maintaining its performance over seven successive cycles without any loss of activity.

2.7 References

1. Galloway W.R.J.D, A. Isidro-Llobet, and D.R. Spring, "Diversity-oriented synthesis as a tool for the discovery of novel biologically active small molecules," *Nat Commun,* **2010**, 1(1), 80.

2. Boberg, M., Jonson, A. C., Leek, H., Jansson-lo, R. & Ashton, M. Chiral Chromatographic Isolation on Milligram Scale of the Human African Trypanosomiasis Treatment. *ACS Omega,* **2020**, 5(37), 23885–23891.

3. Seo, C. S. G. & Morris, R. H. Catalytic Homogeneous Asymmetric Hydrogenation: Successes and Opportunities. *Organometallics,* **2019**, 38, 47−65.

4. Benaglia, M. Recoverable and recyclable chiral organic catalysts. *New J. Chem*., **2006**, 30, 1525–1533.

5. Niknam, K., Saberi, D. & Sefat, M. N. Silica-bonded S -sulfonic acid as a recyclable catalyst for chemoselective synthesis of 1 , 1-diacetates. *Tetrahedron Lett.,* **2009**, 50,

4058–4062.

6.   Chandrasekaran, S. Proline and benzylpenicillin derivatives grafted into mesoporous MCM-41 : Novel organic – inorganic hybrid catalysts for direct. *Indian Acad. Sci.,* **2003**, 115, 365–372.

7.   Soni, J., Sahiba, N., Sethiya, A. & Agarwal, S. Polyethylene glycol : A promising approach for sustainable organic synthesis. *J. Mol. Liq.,* **2020**, 315, 113766.

8.   Zheng, B. *Li J.,* Pathirana C., Qiu S., Schmidt M. A. & Eastgate M. D. Complexation of polyethyleneglycol containing small molecules with magnesium chloride as a purification and isolation strategy. *Org. Process Res. Dev.* **2021**, 25, 2270−2276.

9.   Vekariya, R. H. & Patel, H. D. Polymer supported biodegradable and recyclable. *RSC Adv.* **2015**, 5, 49006–49030.

10.   Clot-Almenara, L., Rodr, C., Osorio-planes, L. & Perica, M. A. Polystyrene-supported TRIP : A highly recyclable catalyst for batch and flow enantioselective allylation of aldehydes. *ACS Catal.* **2016**, 6, 7647−7651.

11.   Giacalone, F., Gruttadauria, M., Marculescu, A. M. & Noto, R. Versatile heterogeneous organocatalysts both for asymmetric aldol reaction in water and α-selenenylation of aldehydes. *Tetrahedron Lett.,* **2007**, 48, 255–259.

12.   Li, J., Yang, G., Qin, Y., Yang, X. & Cui, Y. Recyclable merrifield resin-supported thiourea organocatalysts derived from L -proline for direct asymmetric aldol reaction. *Tetrahedron: Asymmetry,* **2011**, 22, 613–618.

13.   Ni, B. & Headley, A. D. Ionic-Liquid-Supported (ILS) Catalysts for asymmetric organic synthesis. *Chem. Eur. J.,* **2010**, 16, 4426–4436.

14.   Mehnert, C. P., Cook, R. A., Dispenziere, N. C. & Afeworki, M. Supported Ionic Liquid Catalysis - A New Concept for Homogeneous Hydroformylation Catalysis. *J. am. Chem. Soc.,* **2002**, 124, 12932–12933.

15.   Moosavi-zare, A. R., Zolfigol, M. A., Zarei, M., Zare, A. & Afsar, J. Design, characterization and application of silica-bonded imidazolium-sulfonic acid chloride as a novel , active and efficient nanostructured catalyst in the synthesis of hexahydroquinolines. *Appl Catal A,* **2015**, 505, 224-234.

16. Moosavi-zare, A. R., Ali, M., Zarei, M., Zare, A. & Khakyzadeh, V. Application of silica-bonded imidazolium-sulfonic acid chloride (SBISAC) as a heterogeneous nanocatalyst for the domino condensation of arylaldehydes with 2-naphthol and dimedone. *J. Mol. Liq.,* **2015**, 211, 373–380.

17. Bellis, E. & Kokotos, G. Proline-modified poly (propyleneimine) dendrimers as catalysts for asymmetric aldol reactions. *J. Mol. Catal. A,* **2005**, 241, 166–174.

18. Chronopoulos, D. D. *et al.* Conjugating proline derivatives onto multi-walled carbon nanotubes : Preparation , characterization and catalytic activity in water. *Mater. Lett.,* **2015**, 157, 212–214.

19. Ramos-garcés, M. V & Colón, J. L. Preparation of zirconium phosphate nanomaterials and their applications as inorganic supports for the oxygen evolution reaction. *Nanomaterials,* **2020**, 10, 1–18.

20. Gianotti, E., Miletto, I., Ivaldi, C. & Paul, G. Hybrid catalysts based on N-heterocyclic carbene anchored on hierarchical zeolites. *RSC Adv.,* **2019**, 9, 35336–35344.

21. Moma, J. Synthesis and application of pillared clay heterogeneous catalysts for wastewater treatment : A review. *RSC Adv.,* **2018**, 8, 5197–5211.

22. Nagendrappa, G. Organic synthesis using clay and clay-supported catalysts. *Appl. Clay Sci.,* **2011**, 53, 106–138.

23. Nipane, S. V & Gokavi, G. S. Reduced graphene oxide supported silicotungstic acid for efficient conversion of thiols to disulfides by hydrogen peroxide. *Ind. Eng. Chem. Res*., **2014**, 53, 3924−3930.

24. Active, H., Mesoporous, H., Erigoni, A., Rey, F. & Segarra, C. *Catal. Today*., **2019**, 345, 227-236.

25. Emami, M., Bikas, R., Noshiranzadeh, N., Kozakiewicz, A. & Lis, T. Cu(II)-hydrazide coordination compound supported on silica gel as an efficient and recyclable heterogeneous catalyst for green click synthesis of β - hydroxy-1,2,3-triazoles in water. *ACS Omega.,* **2020**, 5, 13344−13357.

26. Helminen, J. & Paatero, E. Inorganic solid supported polymer acid catalyst – Sulfonated polystyrene grafted silica gel in liquid phase esterification. *React. Funct. Polym.,* **2006**, 66, 1021–1032.

27. Jalili F., Zarei M., Zolfigol M.A., Rostamnia S., and Moosavi-zare, R. SBA-15/PrN(CH2PO3H2)2 as a novel and efficient mesoporous solid acid catalyst with phosphorous acid tags and its application on the synthesis of new pyrimido[4,5-bb]quinolones and pyrido[2,3-dd]pyrimidines via anomeric based oxidation. *Microporous Mesoporous Mater.,* **2019**, 294, 109865.

28. Safavi, A., Iranpoor, N. & Saghir, N. Directly silica bonded analytical reagents : synthesis of 2-mercaptobenzothiazole – silica gel and its application as a new sorbent for preconcentration and determination of silver ion using solid-phase extraction method. *Sep. Purif. Technol.,* **2004**, 40, 303–308.

29. Nahum, A. V. L. E. bij, csaba. Surface silanols in silica-bonded hydrocarbonaceous stationary phases ii. irregular retention behavior and effect of sllanol masking. *J. Chromatogr.,* **1981**, 203, 65-84.

30. Esquivel, G. & Rene, I. Method for synthesising heterogeneous solid chiral catalysts and their use in stereoselective reactions. *European Patent,* **2015,** No. EP2732874B1.

31. Kristensen, T. E., Vestli, K., Fredriksen, K. A., Hansen, F. K. & Hansen, T. Synthesis of acrylic polymer beads for organocatalysts. *Org. Lett.* **2009**, 11, 2968-2971.

32. Elmekawy, A. A., Sweeney, J. B. & Brown, D. R. Efficient synthesis of supported proline catalysts for asymmetric aldol reactions. *Catal. Sci. Technol.* **2015**, 5, 690-696.

33. An, Z., Guo, Y., Zhao, L., Li, Z. & He, J. - Proline-grafted mesoporous silica with alternating hydrophobic and hydrophilic blocks to promote direct asymmetric aldol and Knoevenagel−Michael cascade reactions. *ACS Catal.,* **2014**, 4, 2566−2576.

34. Pathak, K. The synthesis of silica-supported chiral BINOL: Application in Ti-catalyzed asymmetric addition of diethylzinc to aldehydes. *J. Mol. Catal. A Chem.,* **2008**, 280, 106–114.

35. Tang, Z. Enantioselective direct aldol reactions catalyzed by L-prolinamide derivatives. *PNAS,* **2004**, 101, 5755–5760.

36. Guan, J. Immobilization of proline onto Al-SBA-15 for C−C bond-forming reactions. *ACS Sustain. Chem. Eng.,* **2014**, 2, 925−933.

37. Vaid, R. & Gupta, M. Silica-l-proline : An efficient and recyclable heterogeneous catalyst for the Knoevenagel condensation between aldehydes and malononitrile in

liquid phase. *Monatsh Chem.,* **2015**, 146, 645-652.

38.   Monge-Marcet, A., Cattoën, X., Alonso, D. A., Nájera, C. & Chi, W. Recyclable silica-supported prolinamide organocatalysts for direct asymmetric aldol reaction in water. *Green Chem.*, **2012**, 14, 1601–1610.

39.   Xavier, F. P. Synthesis and characterization of TiO_2/ SiO_2 nano composites for solar cell applications. *Appl. Nanosci.,* **2012**, 2, 429–436.

40.   Sheykhan, M., Yahyazadeh, A. & Ramezani, L. A novel cooperative Lewis acid / Brønsted base catalyst Fe_3O_4@SiO_2-APTMS-Fe(OH)$_2$: An efficient catalyst for the Biginelli reaction. *Mol. Catal.,* **2017**, 435, 166–173.